

Not All Inputs Are Valid: Towards Open-Set Video Moment Retrieval Using Language

Xiang Fang
Huazhong University of Science and
Technology
Wuhan, China
xfang9508@gmail.com

Wanlong Fang
Huazhong University of Science and
Technology
Wuhan, China
wanlongfang@gmail.com

Daizong Liu
Peking University
Beijing, China
dzliu@stu.pku.edu.cn

Xiaoye Qu
Huazhong University of Science and
Technology
Wuhan, China
xiaoye@hust.edu.cn

Jianfeng Dong
Zhejiang Gongshang University
Guangzhou, China
dongjf24@gmail.com

Pan Zhou
Huazhong University of Science and
Technology
Wuhan, China
panzhou@hust.edu.cn

Renfu Li
Huazhong University of Science and
Technology
Wuhan, China
renfu.li@hust.edu.cn

Zichuan Xu
Dalian University of Technology
Dalian, China
z.xu@dlut.edu.cn

Lixing Chen
Shanghai Jiao Tong University
Shanghai, China
lxchen@sjtu.edu.cn

Panpan Zheng
Xinjiang University
Ürümqi, China
007652@xju.edu.cn

Yu Cheng
The Chinese University of Hong Kong
Hong Kong, China
chengyu05@gmail.com

Abstract

Video Moment Retrieval (VMR) targets to retrieve the specific moment corresponding to a sentence query from an untrimmed video. Although recent works have made remarkable progress in this task, they implicitly are rooted in the closed-set assumption that all the given queries as video-relevant¹. Given an OOD query in open-set scenarios, they still utilize it for wrong retrieval, which might lead to irrecoverable losses in high-risk scenarios, *e.g.*, criminal activity detection. To this end, we creatively explore a brand-new VMR setting termed Open-Set Video Moment Retrieval (OS-VMR), where we should not only retrieve the precise moments based on ID query, but also reject OOD queries. In this paper, we make the first attempt to step toward OS-VMR and propose a novel model **OpenVMR**, which first distinguishes ID and OOD queries based on the normalizing flow technology, and then conducts moment retrieval based on ID

¹In this paper, we treat “video-relevant query” as “in-distribution (ID) query” and “video-irrelevant query” as “out-of-distribution (OOD) query”.

Equal contribution: Xiang Fang, Wanlong Fang and Daizong Liu. Corresponding authors: Pan Zhou and Jianfeng Dong.

Permission to make digital or hard copies of all or part of this work for personal or classroom use is granted without fee provided that copies are not made or distributed for profit or commercial advantage and that copies bear this notice and the full citation on the first page. Copyrights for components of this work owned by others than the author(s) must be honored. Abstracting with credit is permitted. To copy otherwise, or republish, to post on servers or to redistribute to lists, requires prior specific permission and/or a fee. Request permissions from permissions@acm.org.
MM '24, October 28–November 1, 2024, Melbourne, VIC, Australia

© 2024 Copyright held by the owner/author(s). Publication rights licensed to ACM.
ACM ISBN 979-8-4007-0686-8/24/10
<https://doi.org/10.1145/3664647.3680947>

queries. Specifically, we first learn the ID distribution by constructing a normalizing flow, and assume the ID query distribution obeys the multi-variate Gaussian distribution. Then, we introduce an uncertainty score to search the ID-OOD separating boundary. After that, we refine the ID-OOD boundary by pulling together ID query features. Besides, video-query matching and frame-query matching are designed for coarse-grained and fine-grained cross-modal interaction, respectively. Finally, a positive-unlabeled learning module is introduced for moment retrieval. Experimental results on three VMR datasets show the effectiveness of our OpenVMR.

CCS Concepts

• Information systems → Video search.

Keywords

Open-set Video Moment Retrieval, ID Query, OOD Query

ACM Reference Format:

Xiang Fang, Wanlong Fang, Daizong Liu, Xiaoye Qu, Jianfeng Dong, Pan Zhou, Renfu Li, Zichuan Xu, Lixing Chen, Panpan Zheng, and Yu Cheng. 2024. Not All Inputs Are Valid: Towards Open-Set Video Moment Retrieval Using Language. In *Proceedings of the 32nd ACM International Conference on Multimedia (MM '24)*, October 28–November 1, 2024, Melbourne, VIC, Australia. ACM, New York, NY, USA, 11 pages. <https://doi.org/10.1145/3664647.3680947>

1 Introduction

Video Moment Retrieval (VMR) is a challenging yet crucial task in multi-modal retrieval [10, 45, 49–51, 88, 124, 129, 133, 145], which has attracted significant attention in recent years due to its

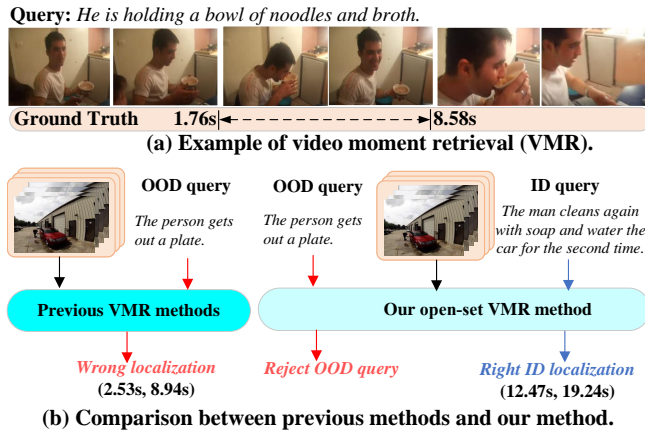


Figure 1: (a) Example of the video moment retrieval (VMR) task. (b) Comparison between previous VMR models and our open-set VMR model. Given a video and a query, previous methods directly conduct retrieval, regardless of whether the query is video-relevant (ID) or video-irrelevant (OOD). Our model can reject OOD queries and recognize ID queries for moment retrieval.

vast potential applications in areas such as human activity retrieval [2, 3, 13–39, 53, 58, 61, 64–67, 73–76, 81, 85, 87, 103, 105, 106, 110–119, 125–127, 143, 144, 147]. As illustrated in Fig. 1(a), its main objective is to identify and retrieve the relevant video moment corresponding to a given sentence query. Obviously, most of the video content is query-irrelevant, and only a very short video segment matches the query. It is substantially more challenging since a well-designed model should not only model the complex multi-modal interaction between videos and queries, but also capture complicated context information for cross-modal semantics alignment. The target model requires recognizing objects/activities and identifying which visual content is sufficient to retrieve the accurate moment expressed in free-form natural language, accounting for the fact that the accurate moment may occupy only a tiny portion of the entire video. To achieve this, both videos and queries must be deeply integrated to distinguish the subtle details of adjacent frames, thereby enabling accurate determination of moment boundaries.

Most existing VMR works [7, 43, 89, 134, 135, 138, 140] are under fully-supervised setting, where each frame is manually labeled as the query-relevant or query-irrelevant frame. Instead of using such dense frame annotations, some recent works try to explore a weakly-supervised setting [8, 69, 92, 104, 146] with only the video-query correspondence to alleviate the reliance on a certain extent. However, their performance is less satisfactory. Although the above VMR methods have made exciting headway, they refer to the close-set assumption that we can obtain a moment in the untrimmed video for any given query. In the real-world open-set environment, we often input a random or irrelevant query for moment retrieval. As shown in Fig. 1(b), given an irrelevant query, previous methods still retrieve a wrong moment as the model output, which will lead to irrecoverable losses in high-risk scenarios, e.g., criminal activity detection. It is unacceptable for our society to classify normal activity as criminal and to treat criminal activity as normal. In real-world multimedia applications, we have a small-scale set of video-query pairs, and many unannotated videos and many video-irrelevant queries. Since labeling video-query annotation is very expensive

and time-consuming, it is unrealistic to manually annotate all the queries as video-relevant (*i.e.*, ID) or video-irrelevant (*i.e.*, OOD).

Therefore, we explore a novel and challenging task: open-set VMR (OS-VMR). Given an untrimmed video, our OS-VMR task aims to not only temporally retrieve the specific moment semantically corresponding to the ID query, but also reject the OOD query shown in Fig. 1(b). Different from previous closed-set settings that only align video and query representations for moment retrieval, our OS-VMR task suffers from three major challenges: 1) *how to accurately learn the distribution of ID queries?* 2) *how to precisely reason the separating boundary of ID and OOD queries?* 3) *how to fully interact with video and ID queries?* In this paper, we propose a novel OpenVMR framework for the challenging OS-VMR task. Specifically, we first design a multi-layer coupling block to construct the normalizing flow for learning ID query distribution based on the multi-variate Gaussian distribution assumption. Besides, we reason the ID-OOD separating boundary by a well-designed uncertainty score and the log-likelihood distribution of each query. Moreover, we pull ID query features together to refine the ID-OOD boundary based on a triplet loss for OOD query detection. After that, for the video and ID query, we conduct the cross-modal interaction for video-query matching and frame-query matching. Finally, we design a simple yet effective positive-unlabeled learning module with pre-defined proposals to retrieve the target moment.

Our main contributions are summarized as follows:

- To the best of our knowledge, we make the first attempt at the open-set Video Moment Retrieval (OS-VMR) task, which is fundamentally more challenging but highly valuable in open-set settings. In this setting, we should not only retrieve the video moment for ID queries, but also reject OOD queries.
- To address our challenging OS-VMR task, we propose a general OpenVMR framework that first distinguishes ID and OOD queries by the normalizing flow technology, and then utilizes ID queries for moment retrieval.
- Experimental results on both open-set and closed-set settings show that our proposed model outperforms other state-of-the-art approaches by a large margin.

2 Related Work

Video moment retrieval. The goal of Video Moment Retrieval (VMR) is to recognize and temporally localize all the action instances in an untrimmed video [7, 70–72, 94, 106, 125, 140]. Most of the existing VMR methods [34–38, 40, 74, 76–83, 86, 87, 87, 134, 142, 145] refer to the fully-supervised setting where all video-query pairs are annotated in detail, including corresponding moment boundaries. The above methods heavily rely on datasets that require numerous manually labeled annotations for training. To ease the human labeling efforts, several recent works [8, 69, 75, 84, 104, 146] consider a weakly-supervised setting that only accesses the information of matched video-query pairs without accurate moment boundaries. However, their performance is significantly worse.

Open-set recognition. Open-set Recognition (OSR) aims to classify in-distribution (ID) samples and reject out-of-distribution (OOD) samples. Previous OSR methods [47, 91, 132, 136] can be divided into four types: 1) Early OSR works [46, 68] refer to a classification framework, which utilizes the maximum softmax probability

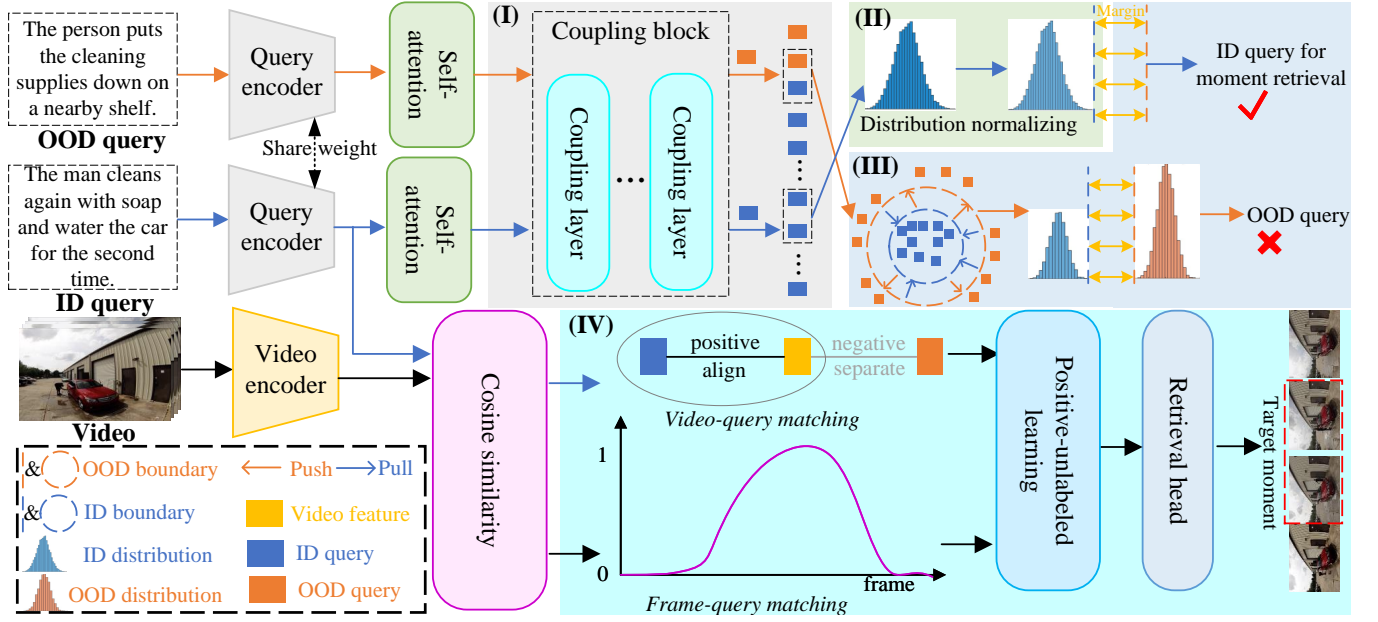


Figure 2: Framework of our method for open-set VMR, where module (I) is “ID knowledge acquisition”, module (II) is “uncertainty-aware OOD boundary reasoning”, module (III) is “ID-OOD boundary refinement”, and module (IV) is “cross-modal interaction”. Best viewed in color.

to determine the ID/OOD samples. 2) Density-based OSR methods [55, 101] are proposed to leverage the probabilistic models for OSR. These methods are under an operating assumption that OOD samples have low likelihoods whereas ID samples have high likelihoods under the estimated density model. 3) Distance-based OSR methods [60, 107] are based on an intuitive idea that OOD samples should be relatively far away from the centroids of ID samples. 4) Reconstruction-based methods [130, 149] often leverage the encoder-decoder framework, which is trained on only ID samples and generates different outcomes for OSR. Inspired by OSR, we step further toward the OS-VMR problem in this paper. Please note that existing OSR methods focus on open-set object detection [48, 52, 96, 120] in the image datasets. These OSR methods cannot effectively understand video and query in our VMR task. However, it is the uniqueness of the moment retrieval in an open-set setting that makes the OS-VMR problem even more challenging and valuable in practice.

3 Our proposed OpenVMR

Setup. Given an untrimmed video V and corresponding language query Q , the traditional Video Moment Retrieval (VMR) task aims to retrieve the query-described activity moment from the video. However, existing VMR methods refer to a closed-set setting, which lacks their understanding of video-irrelevant queries, limiting their real-world information retrieval applications.

To this end, we investigate a more practical but challenging setting, called open-set VMR (OS-VMR), which not only conducts video grounding by the video-relevant query but also rejects the video-irrelevant query. Given an untrimmed video and a sentence query, the OS-VMR task aims to retrieve the moment location from the video (if the query is video-relevant, *i.e.*, ID query), or reject the query (if the query is video-irrelevant, *i.e.*, OOD query). Therefore,

our posed OS-VMR is brand-new and more challenging than VMR. Fig. 2 illustrates the framework of our proposed method.

3.1 Preparation

Video encoder. Following previous VMR works [140, 142, 145], given a video with N_v frames, we first extract its frame-wise features by a pre-trained C3D network [108], and then employ a multi-head self-attention [109] module to capture the long-range dependencies among video frames. We denote the extracted video features as $V = \{v_i\}_{i=1}^{N_v} \in \mathbb{R}^{N_v \times d}$, where d is feature dimension.

Query encoder. Similarly, given a query with N_w words, we also follow previous VMR works [140, 142, 145] to utilize the Glove [98] embedding to encode each word into dense vector. We further employ the Bi-GRU [9] layers to extract word-level query feature $W = \{w_j\}_{j=1}^{N_w} \in \mathbb{R}^{N_w \times d}$. To capture the global semantics of the whole query, we utilize the Skip-thought parser [56] to extract the sentence-level query feature $q \in \mathbb{R}^d$.

3.2 ID Knowledge Acquisition

When it comes to detecting OOD queries, we aim to find an OOD-independent separating boundary to distinguish ID queries and OOD queries. Thus, we extract the simplified distribution of ID query features. We use normalizing flow [11, 12, 59, 97, 131] to learn the distribution of ID query features. In a VMR dataset, for a video, we select N_{id} ID queries and N_{ood} OOD queries. We refer to the sentence-level query features extracted by the query encoder as input features for normalizing flow. We denote these features as $Q = Q^{id} \cup Q^{ood}$, where $Q^{id} = \{q_i^{id}\}_{i=1}^{N_{id}}$ and $Q^{ood} = \{q_j^{ood}\}_{j=1}^{N_{ood}}$ are ID and OOD query features, respectively.

3.2.1 Normalizing Flow Construction. Firstly, we denote $\Phi_\omega : Q \in \mathbb{R}^d \rightarrow X \in \mathbb{R}^d$ as our normalizing flow, where ω is a learnable parameter and X denotes the latent space. Especially, a coupling

block with multiple coupling layers [11] is leveraged such that $\Phi_\omega = \Phi_C \circ \dots \circ \Phi_2 \circ \Phi_1$, where C is the total layer number.

Defining d -dimensional input and output features of normalizing flow as $k_0 = q \in \mathcal{Q}$ and $k_C = x \in \mathcal{X}$, the output of the c -th latent layer is $k_c = \Phi_c(k_{c-1})$, where $\{k_c\}_{c=1}^{C-1}$ are the intermediate outputs. By the change of variables formula, the input distribution estimated by model $p_\omega(q)$ can be formulated as:

$$\log p_\omega(q) = \sum_{c=1}^C \log |\det J_{\Phi_c}(k_{c-1})| + \log p_{\mathcal{X}}(\Phi_\omega(q)), \quad (1)$$

where $J_{\Phi_c}(k_{c-1}) = \partial \Phi_c(k_{c-1}) / \partial k_{c-1}$ is the Jacobian matrix of Φ_c at k_{c-1} , and \det means determinant. Besides, we can approximate the feature distribution $p_{\mathcal{Q}}$ with $p_\omega(q)$ by the normalizing flow.

By optimizing the log-likelihoods across the training distribution $p_{\mathcal{Q}}$, we can obtain the set of parameters ω as follows:

$$\omega^* = \underset{\omega}{\operatorname{argmin}} \mathbb{E}_{q \sim p_{\mathcal{Q}}} [-\log p_\omega(q)]. \quad (2)$$

3.2.2 Learning ID Query Feature Distribution. Then, by maximum likelihood optimization, we leverage the normalizing flow to learn ID query feature distribution. In general, the latent variable distribution $p_{\mathcal{X}}(x)$, $x \in \mathbb{R}^d$ can be assumed to obey the following multi-variate Gaussian distribution [44]:

$$p_{\mathcal{X}}(x) = (2\pi)^{-\frac{d}{2}} \det(\sigma^{-\frac{1}{2}}) \exp[-\frac{1}{2}(x - \mu)^\top \sigma^{-1}(x - \mu)], \quad (3)$$

where μ and σ are the mean and the covariance, respectively. For simplicity, we assume the latent variables for the ID query feature to obey the standard normal distribution during training. By replacing $p_{\mathcal{X}}(x) = (2\pi)^{-\frac{d}{2}} \exp(-\frac{1}{2}x^\top x)$ in Eq. (1), we rewrite the optimization objective in Eq. (2) as follows:

$$\omega^* = \underset{\omega}{\operatorname{argmin}} \mathbb{E}_{q \sim p_{\mathcal{Q}}} \left[\frac{1}{2} \Phi_\omega(q)^\top \Phi_\omega(q) - \sum_{c=1}^C \log |\det J_{\Phi_c}(k_{c-1})| \right]. \quad (4)$$

Since $d/2 \log(2\pi)$ is constant, we remove it in Eq. (4). To learn the ID query feature distribution, we define the maximum likelihood loss function as follows:

$$\mathcal{L}_1 = \mathbb{E}_{q \in \mathcal{Q}^{id}} \left[\frac{1}{2} \Phi_\omega(q)^\top \Phi_\omega(q) - \sum_{c=1}^C \log |\det J_{\Phi_c}(k_{c-1})| \right]. \quad (5)$$

3.3 OOD Boundary Reasoning

Based on the learned ID query feature distribution, we can search an explicit and compact separating boundary between ID and OOD query. To reduce the computational cost from high-dimensional query features, we consider searching the boundary based on the uncertainty score. Since the log-likelihoods generated by the normalizing flow can be equivalently converted to uncertainty scores, we select the boundary on the log-likelihood distribution.

3.3.1 Uncertainty Score. By the normalizing flow, we can estimate the exact log-likelihood $\log p(q)$ for each query feature q :

$$\log p(q) = \sum_{c=1}^C \log |\det J_{\Phi_c}(k_{c-1})| - \frac{1}{2} \Phi_\omega(q)^\top \Phi_\omega(q). \quad (6)$$

With the estimated log-likelihood $\log p(q)$, we utilize the exponential function to convert it to likelihood. Since we aim to maximize log-likelihoods for normal features in Eq. (5), the likelihood can directly measure the uncertainty. Thus, we can obtain the following uncertainty score: $u(q) = \max_{q' \in \mathcal{Q}} (\exp(\log p(q')) - \exp(\log p(q)))$, where $u(q)$ is the uncertainty score of query q . The log-likelihood can be equivalently converted to the uncertainty score since the

exponential function is monotonic. Therefore, the boundary in uncertainty score distribution is equivalent to the separating boundary in log-likelihood distribution.

3.3.2 Reasoning ID-OOD Separating Boundary. With log-likelihood distribution, we can search the separating boundary as follows: 1) Firstly, we search the ID log-likelihood distribution by ID log-likelihoods $\mathcal{P}_{id} = \{\log p_i\}_{i=1}^{N_{id}}$ based on the log-likelihood estimation formulation in Eq. (6). 2) Then, we can approximate the log-likelihood distribution of all ID queries by \mathcal{P}_{id} . 3) After that, we introduce a position hyper-parameter α to determine the boundary. Specially, we set the α -th percentile (e.g., $\alpha = 5$) of sorted ID log-likelihood distribution as the ID boundary b_{id} , which also serves as the upper bound of the ID false positive rate is $\alpha\%$. 4) To enhance the robustness of our model, we employ the margin hyper-parameter Δ and define an OOD boundary as $b_{ood} = b_{id} - \Delta$.

3.4 ID-OOD Boundary Refinement

With the explicit ID-OOD boundary, we design an ID-OOD boundary refinement module for discriminative feature learning. Then, we use the boundary b_{id} as the contrastive target. Specially, we push OOD query features whose log-likelihoods are larger than b_{ood} apart from b_{id} at least beyond the margin Δ , while pulling together ID query features whose log-likelihoods are smaller than b_{id} . Thus, we introduce the following triplet loss:

$$\mathcal{L}_2 = \sum_{i=1}^{N_{id}} |\min((\log p_i - b_{id}), 0)| + \sum_{j=1}^{N_{ood}} |\max((\log p_j - b_{id} + \Delta), 0)|. \quad (7)$$

Since any log-likelihood $\log p_i$ fallen into the margin region (b_{ood}, b_{id}) will increase the value of \mathcal{L}_2 , we can encourage the sparse log-likelihood distribution in the margin region (b_{ood}, b_{id}) . The log-likelihoods can range from a large region $(-\infty, 0]$, which makes it difficult to select the satisfactory hyper-parameter Δ . To normalize the log-likelihoods to the small range (e.g., $[-1, 0]$), we introduce a large enough normalizer h_{id} (e.g., $h_{id} = 100$). Since these log-likelihoods can be easily divided into OOD queries, the extremely small log-likelihoods (less than -1) can be excluded outside the loss in Eq. (7). Thus, minimizing the loss in Eq. (7) will encourage all log-likelihoods \mathcal{P} to distribute in the regions $[-1, b_{ood}]$ or $[b_{id}, 0]$.

Given a query, if its log-likelihood falls into $[b_{id}, 0]$, we treat it as ID. Otherwise, it is OOD.

3.5 Cross-modal Interaction and Training

3.5.1 Video-query Matching. The frame-level video and word-level query representations are denoted as $V \in \mathbb{R}^{N_v \times d}$ and $W \in \mathbb{R}^{N_w \times d}$, respectively. Specially, we first extract the global representation by an attentive pooling: $v' = \sum_{i=1}^{N_v} f_i^v v'_i$, $f^v = \xi_{\text{softmax}}(VM_v)$, $q' = \sum_{j=1}^{N_w} f_j^q q'_j$, $f^q = \xi_{\text{softmax}}(WM_q)$, where $M_v \in \mathbb{R}^{d \times 1}$ and $M_q \in \mathbb{R}^{d \times 1}$ are learnable matrices; v' and q' are global video and query representations, respectively. To evaluate the video-query matching score, we introduce the following cosine similarity: $\text{Sim}(v', q') = v'^\top \cdot q' / (\|v'\|_2 \|q'\|_2)$, where $\|\cdot\|_2$ denotes the L2-norm of a vector.

In a training batch with N_b video-query pairs $\{V_i, Q_i\}_{i=1}^{N_b}$, we adopt the multi-modal features $\{v'_i, q'_i\}_{i=1}^{N_b}$ for cross-modal semantic alignment. For positive and negative video-query pairs, we utilize the video-query matching score $\text{Sim}(v', q')$ for the following

alignment loss: $\mathcal{L}_3 = -\frac{1}{|N_b|} \sum_{i=1}^{N_b} \log \frac{\exp(\text{Sim}(v'_i, q'_i)/\eta)}{\sum_{i \neq j} \exp(\text{Sim}(v'_i, q'_j)/\eta)}$, where η is a temperature parameter.

3.5.2 Frame-query Matching. To further better understand the given video V and ID query Q^{id} , we design a **Frame-Query Matching (FQM)** module to estimate the matching videos and queries based on the likelihood of each frame about queries.

Specially, the FQM module includes two linear layers followed by two functions (sigmoid and tanh), which is defined as: $\text{FQM}(f_i^v, q') = \xi_{\text{sigmoid}}(\xi_{\text{tanh}}(f_i^v M_1) q' M_2)$, where $\xi_{\text{sigmoid}}(\cdot)$ and $\xi_{\text{tanh}}(\cdot)$ denote sigmoid and tanh functions, respectively; f_i^v denotes the i -th frame feature in video V ; $M_1 \in \mathbb{R}^{d \times 1}$ and $M_2 \in \mathbb{R}^{d \times 1}$ are learnable matrices. We denote the likelihood of each frame about q' as $P(f_i^v | q')$. Also, we can obtain the probability: $P(f_i^v | q') = \text{FQM}(f_i^v, q')$.

Then, we calculate the frame-aware attention scores a by the softmax function as: $a = \xi_{\text{softmax}}(p_1, p_2, \dots, p_{N_v})$, where $\xi_{\text{softmax}}(\cdot)$ denotes the softmax function. Based on a , we can enhance the frame-level feature f_i^v : $\hat{f}_i^v = a \odot f_i^v$, where \odot denotes an element-wise product and \hat{f}_i^v is the enhanced frame features. After obtaining \hat{f}_i^v , we further integrate it with multi-level query features as: $f_i^{\text{fuse}} = M_3 \hat{f}_i^v + M_4 \sum_{j=1}^{N_w} w_j + M_5 q'$, where f_i^{fuse} is the fused feature, and M_3, M_4 and M_5 are learnable weight matrices.

3.5.3 Positive-unlabeled Learning. Since most of the video content is background, it is significant to predict the foreground frames that are relevant to the ID query. We can treat query-relevant frames as positive data, whereas query-irrelevant frames are unlabeled data. We can transfer the VMR problem to a semi-supervised learning problem, positive-unlabeled learning (PUL) [1]. Thus, we design a simple yet effective PUL module to predict the target moment.

Specifically, we follow previous VMR works [145] to retrieve the target moment with pre-defined moment proposals based on f_i^{fuse} , where we sample t proposals for each frame. Then, we obtain the similarity score $s_i \in [0, 1]$ between the ID query and the i -th proposal. In a training batch $\mathcal{S} = \{s_i\}$, we can divide these proposals into two sets: positive set $\overline{\mathcal{P}} = \{s_i | s_i \geq 0.5\}$ and the unlabeled background set $\overline{\mathcal{U}} = \{s_i | s_i < 0.5\}$. Therefore, we ascendingly sort $\overline{\mathcal{U}}$ and select top- N_s samples to form the most likely negative set $\overline{\mathcal{N}} = \{s_i | s_i \in \text{sort}(\overline{\mathcal{U}})_{1, \dots, N_s}\}$. Since $|\overline{\mathcal{U}}| \gg |\overline{\mathcal{P}}|$ in most batches, we set $N_s = |\overline{\mathcal{N}}| := \min(|\overline{\mathcal{P}}|, |\overline{\mathcal{U}}|)$ for smooth training. Finally, we employ the binary cross-entropy loss based on the positive set $\overline{\mathcal{P}}$ and the negative set $\overline{\mathcal{N}}$:

$$\mathcal{L}_{\text{BCE}} = -\frac{1}{|\overline{\mathcal{P}}|} \sum_{s_i \in \overline{\mathcal{P}}} \log s_i - \frac{1}{|\overline{\mathcal{N}}|} \sum_{s_i \in \overline{\mathcal{N}}} \log(1 - s_i). \quad (8)$$

By Eq. (8), we can push the probably pure background proposals far away from positive proposals. Although the PUL method is simple, the learned similarity scores are enough for distinguishing the foreground and background proposals.

As the boundaries of pre-defined proposals are coarse, we employ a retrieval regression loss for calibrating the retrieval. We calculate the regression loss for every positive sample:

$$\mathcal{L}_{\text{reg}} = \frac{1}{|\overline{\mathcal{P}}|} \sum \mathcal{L}_{\text{smooth}}(t_s, t'_s) + \mathcal{L}_{\text{smooth}}(t_e, t'_e), \quad (9)$$

where $\mathcal{L}_{\text{smooth}}$ is the smooth L_1 loss; t_s, t_e are the ground-truth start and end timestamps; t'_s, t'_e are the predicted timestamps.

Table 1: Closed-set datasets and open-set datasets during training and testing, where ‘‘ANC’’ denotes ‘‘ActivityNet Captions’’, ‘‘CS’’ denotes ‘‘Charades-STA’’, and ‘‘All’’ denotes all three datasets.

Dataset	Closed-set train		Closed-set test		Open-set train		Open-set test	
	Video	Query	Video	Query	Video	Query	Video	Query
ANC	ANC	ANC	ANC	ANC	ANC	ANC	ANC	All
CS	CS	CS	CS	CS	CS	CS	CS	All
TACoS	TACoS	TACoS	TACoS	TACoS	TACoS	TACoS	TACoS	All

For convenience, we set $\mathcal{L}_4 = \mathcal{L}_{\text{BCE}} + \mathcal{L}_{\text{reg}}$. Therefore, we can obtain the following overall loss:

$$\mathcal{L} = \mathcal{L}_1 + \lambda_1 \mathcal{L}_2 + \lambda_2 \mathcal{L}_3 + \lambda_3 \mathcal{L}_4, \quad (10)$$

where λ_1, λ_2 and λ_3 are the balanced weight hyper-parameters.

Inference. Given a video and a sentence query, we first feed them into our model to detect if the query is ID or OOD. If the query is ID, we can obtain the fused cross-modal feature f_i^{fuse} . Then, we predict the moment boundary (t'_s, t'_e) in Eq. (9). ‘‘Top- n (R@ n)’’ moment candidates will be selected with non-maximum suppression [95].

4 Experiments

4.1 Datasets and Evaluation Metrics

Datasets. We experiment on four VMR datasets with various characteristics: Charades-STA [40], Activitynet-Captions [57] and TACoS [99]. In this paper, we conduct experiments under two settings: closed-set and open-set, whose split principle is illustrated in Table 1. In the closed-set setting, for each dataset, we utilize its queries and its videos for both training and testing. In the open-set setting, we train each dataset based on its queries and videos, while we conduct testing on its videos and queries from all three datasets.

ActivityNet Captions. ActivityNet Captions is introduced by [57], which contains about 20k untrimmed videos and 100k descriptions with diverse open-domain activities. Following the split principle in [142], in the closed setting, we utilize 37,417 video-query pairs for training, and 34,536 pairs for testing, respectively.

Charades-STA. It is built on Charades [102] by [40], including 9,848 videos of indoor scenarios. In the closed setting, we use 12,408 and 3,720 video-sentence pairs for training and testing, respectively.

TACoS. TACoS is a challenging dataset collected from the MPII Cooking Composite Activities [100], which contains 127 long videos of cooking scenarios. In the closed setting, we follow the standard split used in [40] and obtain 10,146, and 8,672 video-sentence pairs as training and testing dataset, respectively.

Evaluation metrics. There are two challenges in our method: *ID query for moment retrieval* and *OOD query detection*. Thus, we use two types of metrics for comprehensive performance evaluation: 1) *ID query for moment retrieval*. Following [40, 140], we adopt ‘‘R@ n , IoU= m ’’ as the evaluation metric, which denotes the percentage of language queries having at least one result whose Intersection over Union (IoU) with ground truth is larger than m in top- n retrieved moment. In our experiments, we use $n \in \{1, 5\}$ for all datasets, $m \in \{0.5, 0.7\}$ for Charades-STA, $m \in \{0.3, 0.5\}$ for ActivityNet Captions and TACoS. 2) *OOD query detection*. To evaluate open-set performance, we introduce two popular metrics to evaluate the performance of detecting ID and OOD queries for a given video: the Area Under the Receiver Operating Characteristic (**AUROC**) curve and the Area Under the Precision-Recall (**AUPR**) [90]. For all the metrics, the larger value denotes better performance.

Table 2: Effectiveness comparison for closed-set VMR.

ActivityNet Captions					
Method	Type	R@1, IoU=0.3	R@1, IoU=0.5	R@5, IoU=0.3	R@5, IoU=0.5
CTRL [40]	FS	-	29.01	-	59.17
2D-TAN [142]	FS	59.45	44.51	85.53	77.13
DRN [137]	FS	-	45.45	-	77.97
RaNet [41]	FS	-	45.59	-	75.93
MIGCN [141]	FS	-	48.02	-	78.02
MMN [123]	FS	65.05	48.59	87.25	79.50
G2L [62]	FS	-	51.68	-	81.32
ICVC [6]	WS	46.62	29.52	80.92	66.61
LCNet [128]	WS	48.49	26.33	82.51	62.66
VCA [122]	WS	50.45	31.00	71.79	53.83
WSTAN [121]	WS	52.45	30.01	79.38	63.42
CNM [148]	WS	55.68	33.33	-	-
Ours	OS	69.85	56.47	94.38	86.54
Charades-STA					
Method	Type	R@1, IoU=0.5	R@1, IoU=0.7	R@5, IoU=0.5	R@5, IoU=0.7
CTRL [40]	FS	23.62	8.89	58.92	29.52
MMN [123]	FS	47.31	27.28	83.74	58.41
2D-TAN [142]	FS	39.81	23.25	79.33	52.15
RaNet [41]	FS	43.87	26.83	86.67	54.22
DRN [137]	FS	45.40	26.40	88.01	55.38
G2L [62]	FS	47.91	28.42	84.80	59.33
MomentDiff [63]	FS	53.79	30.18	-	-
WSTAN [121]	WS	29.35	12.28	76.13	41.53
ICVC [6]	WS	31.02	16.53	77.53	41.91
CNM [148]	WS	35.15	14.95	-	-
VCA [122]	WS	38.13	19.57	78.75	37.75
LCNet [128]	WS	39.19	18.17	80.56	45.24
Ours	OS	58.38	33.53	93.62	62.35
TACoS					
Method	Type	R@1, IoU=0.3	R@1, IoU=0.5	R@5, IoU=0.3	R@5, IoU=0.5
CTRL [40]	FS	18.32	13.30	36.69	25.42
ACRN [88]	FS	19.52	14.62	34.97	24.88
CMIN [145]	FS	24.64	18.05	38.46	27.02
SCDM [134]	FS	26.11	21.17	40.16	32.18
DRN [137]	FS	-	23.17	-	33.36
2D-TAN [142]	FS	37.29	25.32	57.81	45.04
MMN [123]	FS	39.24	26.17	62.03	47.39
FVMR [42]	FS	41.48	29.12	64.53	50.00
G2L [62]	FS	42.74	30.95	65.83	49.86
RaNet [41]	FS	43.34	33.54	67.33	55.09
MomentDiff [63]	FS	44.78	33.68	-	-
Ours	OS	55.44	42.72	73.48	64.48

Implementation details. For the video encoder, we apply C3D [108] to encode the videos on ActivityNet Caption and I3D [4] on Charades-STA and TACoS. Since some videos are overlong, we set the length of frame sequences M to 64, 64 and 200 for Charades-STA, ActivityNet Captions and TACoS, respectively. For the query encoder, we utilize GloVe 840B 300d [98] to embed each word as word features. We sample 800 moment proposals for TACoS and 384 for Charades-STA and ActivityNet Captions similar with [145]. We train our model for 200 epochs with a batch size of 128 and an early stopping strategy. Parameter optimization is performed by Adam [54] optimizer with a learning rate of 0.0008. We conduct our experiments on a single Nvidia TITAN XP GPU.

4.2 Comparison with State-of-the-Arts

4.2.1 Compared Methods. We conduct performance comparison on all three datasets with official train/test splits under closed-set and open-set settings. To evaluate efficiency, we only choose the open-source compared methods: (i) **Fully-supervised (FS)** setting [40–42, 62, 63, 88, 123, 134, 137, 141, 142, 145]; (ii) **Weakly-supervised (WS)** setting [6, 121, 122, 128, 146, 148]. For convenience, we denote our posed “**open-set setting**” as “**OS**”. Following [93, 139], we directly cite the results of compared methods from corresponding works. The best results are **bold**.

4.2.2 Closed-set Evaluation. The quantitative comparison results of our model and compared methods on ActivityNet Captions, Charades-STA, and TACoS are reported in Table 2.

Based on these experimental results, we list several notable observations as follows: 1) Compared with other state-of-the-art methods, our proposed model achieves the highest performance over all metrics on three datasets, which demonstrates the superiority of our proposed model. 2) On the ActivityNet Captions dataset, our model outperforms all the compared methods over all metrics. Particularly, our model beats the best compared fully-supervised method G2L by 5.22% in terms of “R@5, IoU=0.5”. As for the best compared weakly-supervised method CNM, our model outperforms it by 14.17% over “R@1, IoU=0.3”. It shows that our model has excellent generalization ability in more complex and diverse real-world scenarios by frame-query matching and video-query matching. 3) On the Charades-STA dataset, based on the reported settings of previous methods, our proposed method reaches the new state-of-the-art on all the metrics. 4) On the TACoS dataset, our model surpasses other state-of-the-art methods by a large margin.

4.2.3 Open-set Evaluation. Similarly, we conduct open-set experiments on all three datasets. Table 3 shows the open-set VMR performance on ActivityNet Captions, Charades-STA, and TACoS respectively, where Ours(a), Ours(b) and Ours(c) are our three ablation models, Ours(full) is our full model. Obviously, our model achieves the best performance on three datasets over all the metrics.

Open-set results on ActivityNet Captions: Particularly, our model beats the best compared fully-supervised method MMN by 15.79% in terms of “R@1, IoU=0.5”. As for the best compared weakly-supervised method CNM, our model outperforms it by 23.01% over “R@1, IoU=0.3”. The main reason is that compared methods cannot distinguish ID and OOD queries, and directly utilize OOD queries for VMR, which significantly reduces their performance under the realistic open-set setting. On the contrary, we can correctly recognize OOD queries and precisely retrieve the target moment by ID queries, which illustrates the effectiveness of our method.

Open-set results on Charades-STA: On the Charades-STA dataset, our method achieves the best results in all the cases. This is because the Charades-STA dataset is under the indoor scenarios, which are irrelevant to outdoor queries in other two datasets. Previous methods directly retrieve outdoor moments based on outdoor queries, leading to unreasonable retrieval results for the open-set VMR task. **Open-set results on TACoS:** On the TACoS dataset, our model outperforms the best compared method MomentDiff by 24.14% and 12.21% over “R@1, IoU=0.3” and “R@1, IoU=0.5”, respectively. The main reason for the significant performance improvement is that all

Table 3: Effectiveness comparison for open-set VMR.

ActivityNet Captions					
Method	Type	R@1, IoU=0.3	R@1, IoU=0.5	AUROC	AUPR
CTRL [40]	FS	22.16	13.42	-	-
2D-TAN [142]	FS	30.88	22.95	-	-
DRN [137]	FS	31.75	26.34	-	-
RaNet [41]	FS	30.96	28.43	-	-
MIGCN [141]	FS	32.40	29.57	-	-
MomentDiff [63]	FS	29.59	30.17	-	-
MMN [123]	FS	35.17	29.92	-	-
ICVC [6]	WS	18.43	10.76	-	-
LCNet [128]	WS	20.48	11.69	-	-
VCA [122]	WS	21.50	10.36	-	-
WSTAN [121]	WS	24.76	12.38	-	-
CNM [148]	WS	28.44	15.74	-	-
Ours(a)	OS	42.15	30.03	33.20	38.87
Ours(b)	OS	45.02	31.72	32.48	37.39
Ours(c)	OS	48.68	36.84	38.16	41.80
Ours(full)	OS	50.96	38.75	39.24	43.68
Charades-STA					
Method	Type	R@1, IoU=0.5	R@1, IoU=0.7	AUROC	AUPR
CTRL [40]	FS	9.16	2.35	-	-
MMN [123]	FS	21.85	10.43	-	-
2D-TAN [142]	FS	16.46	8.13	-	-
MomentDiff [63]	FS	12.68	7.26	-	-
RaNet [41]	FS	18.50	9.77	-	-
DRN [137]	FS	20.13	8.10	-	-
WSTAN [121]	WS	8.15	3.92	-	-
ICVC [6]	WS	10.40	2.97	-	-
CNM [148]	WS	11.43	6.28	-	-
VCA [122]	WS	14.72	5.71	-	-
LCNet [128]	WS	13.52	7.39	-	-
Ours(a)	OS	28.40	16.77	32.02	35.63
Ours(b)	OS	30.27	15.29	33.82	34.95
Ours(c)	OS	33.18	19.05	36.75	39.86
Ours(full)	OS	34.62	19.58	38.76	40.29
TACoS					
Method	Type	R@1, IoU=0.3	R@1, IoU=0.5	AUROC	AUPR
CTRL [40]	FS	11.95	6.42	-	-
ACRN [88]	FS	14.28	9.55	-	-
CMin [145]	FS	13.84	10.16	-	-
SCDM [134]	FS	14.48	10.67	-	-
DRN [137]	FS	15.73	11.05	-	-
2D-TAN [142]	FS	14.80	11.13	-	-
MMN [123]	FS	17.64	11.52	-	-
FVMR [42]	FS	14.83	10.10	-	-
MomentDiff [63]	FS	16.28	12.34	-	-
RaNet [41]	FS	13.72	9.45	-	-
MIGCN [141]	FS	14.13	11.39	-	-
Ours(a)	OS	33.81	19.76	38.63	34.82
Ours(b)	OS	35.48	20.87	37.31	35.29
Ours(c)	OS	36.54	22.47	40.82	35.96
Ours(full)	OS	38.27	23.60	41.95	37.80

the videos on TACoS are cooking-related, which only corresponds to cooking-related queries. Given some cooking-irrelevant OOD queries from other two datasets, previous methods mistakenly utilize these OOD queries for wrong moment retrieval, which severely limits their performance.

Table 4: Efficiency comparison for closed-set VMR on TACoS.

Method	Run-Time	Model Size	R@1, IoU=0.5
ACRN [88]	5.96s	128M	14.62
CTRL [40]	3.58s	22M	13.30
TGN [5]	0.89s	166M	18.90
2D-TAN [142]	0.71s	232M	25.32
DRN [137]	0.22s	214M	23.17
MomentDiff [63]	1.85s	248M	33.68
Ours	0.08s	92M	39.72

4.2.4 Efficiency Comparison. In Table 4, we evaluate the efficiency of our proposed model, by fairly comparing its running time and model size in the inference phase with existing open-source methods on TACoS. Obviously, we achieve much faster processing speeds with relatively fewer learnable parameters. This attributes to: 1) Proposal-based methods (ACRN, CTRL, TGN, 2D-TAN, DRN) suffer from the time-consuming proposal-matching process. Unlike them, our retrieval module utilizes the positive-unlabeled learning module, which is much more efficient. 2) Different from them, our model only learns an effective and efficient retrieval backbone without introducing additional parameters during inference.

4.2.5 Visualization. Fig. 3 depicts the retrieval visualizations on ActivityNet Captions under both closed-set and open-set settings. In the closed-set setting, our model achieves better retrieval performance than previous state-of-the-art methods (MMN and WSTAN). This is because our model can fully conduct cross-modal interaction by both video-query matching and frame-query matching. For the challenging open-set setting, our model can reason the right ID-OOD boundary for OOD query recognition, thus rejecting video-irrelevant queries.

4.3 Ablation Study and Analysis

Main ablation studies. To demonstrate the effectiveness of each component in our model, we conduct ablation studies regarding the components (*i.e.*, ID knowledge acquisition module, uncertainty-aware OOD boundary reasoning module and ID-OOD boundary refinement module). In particular, we remove each key individual module to investigate its contribution. For convenience, we design three ablation models: 1) Ours(a). We remove the ID knowledge acquisition module while keeping the other two modules. 2) Ours(b). We remove the uncertainty-aware OOD boundary reasoning module while keeping the other two modules. 3) Ours(c). We remove the ID-OOD boundary refinement module while keeping the other two modules. Besides, we use our full model as the baseline: Ours(full). Since we focus on the open-set setting, we conduct corresponding experiments in Table 3. Based on these tables, we can observe that all three modules contribute a lot to the final performances on all three datasets, demonstrating their effectiveness in the open-set VMR task. As the core module for detecting OOD queries, the ID knowledge acquisition module brings the greatest improvement, illustrating that it provides ID distribution information for ID boundary reasoning. Also, the uncertainty-aware OOD boundary reasoning module achieves significant performance improvement, which illustrates the effectiveness of our uncertainty score and OOD boundary reasoning. Besides, the ID-OOD boundary refinement module improves performance in all metrics.

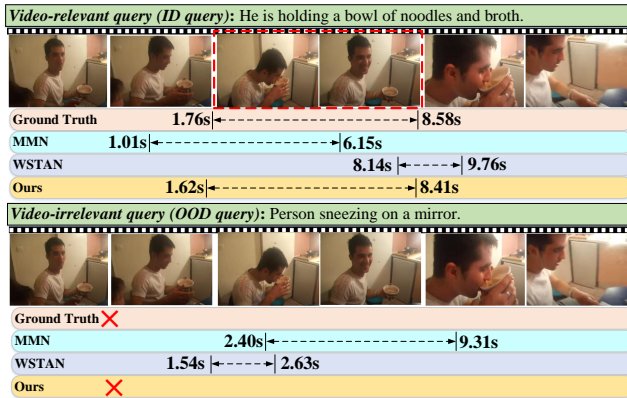


Figure 3: Visualization results on ActivityNet Captions (top: closed-set, bottom: open-set), where “ \times ” means “reject the query”.

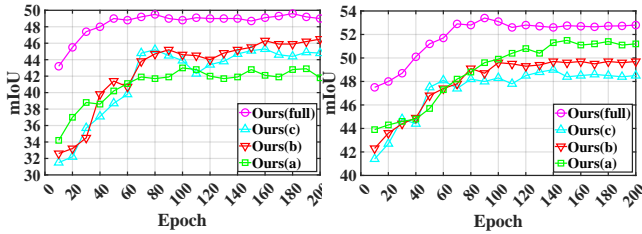


Figure 4: Training performance of each ablation module for open-set VMR on ActivityNet Captions (left) and Charades-STA (right).

Table 5: Effect of ID Knowledge Acquisition (IKA), Uncertainty-aware OOD Boundary Reasoning (UOBR) and ID-OOD Boundary Refinement (IBR) for open-set VMR on Charades-STA, where “DD” means “Dirichlet Distribution”, “MGD” means “Multi-variate Gaussian Distribution” and “MD” means “Multinomial Distribution”.

Module	Changes	R@1, IoU=0.5	R@1, IoU=0.7	AUROC	AUPR
IKA	C=5	33.87	19.21	38.08	39.22
	C=6	34.62	19.58	38.76	40.29
	C=7	34.18	19.04	38.96	40.23
	DD	33.14	16.38	35.71	38.55
	MGD	34.62	19.58	38.76	40.29
UOBR	MD	31.42	15.80	34.33	39.12
	$\alpha = 4$	34.24	18.52	38.01	40.10
	$\alpha = 5$	34.62	19.58	38.76	40.29
IBR	$\alpha = 6$	33.73	19.41	37.95	40.20
	$\Delta = 0.03$	34.23	18.02	37.15	39.86
	$\Delta = 0.04$	34.62	19.58	38.76	40.29
	$\Delta = 0.05$	34.34	18.60	38.12	39.39

Training process of different ablation models. Following [69], we analyze the training process and retrieval performance of different ablation models in Fig. 4. We can obtain the following representative observations: (i) During training, Our(full) outperforms other ablation models, which further demonstrates the effectiveness of each module. (ii) Our(full) converges faster than ablation models, which shows that our full model is more efficient on time-consuming. Thus, our full model can process these challenging datasets more efficiently.

Effect of ID knowledge acquisition. In the ID knowledge acquisition (IKA) module, we design a multi-layer coupling block and utilize the multi-variate Gaussian distribution (MGD). We implement different variants of the IKA module in Table 5. Obviously, we can achieve the best performance when we utilize the five-layer

Table 6: Ablations on cross-modal interaction for open-set VMR on ActivityNet Captions, where “VQM” means “video-query matching”, “FQM” means “frame-query matching”, “PUL” means “positive-unlabeled learning”.

Ablation	R@1, IoU=0.5	R@1, IoU=0.7	AUROC	AUPR
w/o VQM	47.93	35.40	35.92	41.25
w/o FQM	48.50	37.02	37.06	42.54
w/o PUL	48.17	36.64	36.56	41.86
Ours(full)	50.96	38.75	39.24	43.68

Table 7: Parameter analysis on ActivityNet Captions.

Parameter	Changes	R@1, IoU=0.5	R@1, IoU=0.7	AUROC	AUPR
λ_1	0.5	50.28	38.12	38.06	42.39
	0.6	50.96	38.75	39.24	43.68
	0.7	49.81	38.10	38.94	43.51
λ_2	0.2	50.26	38.89	38.72	40.13
	0.3	50.96	38.75	39.24	43.68
λ_3	0.4	50.11	38.24	38.50	42.18
	0.6	50.16	37.87	38.25	42.75
η	0.7	50.96	38.75	39.24	43.68
	0.8	51.29	38.86	38.95	42.94
η	0.1	50.36	38.28	38.77	43.92
	0.2	50.96	38.75	39.24	43.68
	0.3	50.29	38.15	38.76	43.10

coupling block and MGD to learn ID distribution. It demonstrates that the five-layer coupling block can sufficiently construct the normalizing flow and learn ID query feature distribution based on multi-variate Gaussian distribution assumption.

Analysis on uncertainty-aware OOD boundary reasoning. Similarly, we conduct ablation on the uncertainty-aware OOD boundary reasoning (UOBR) module. As shown in Table 5, we change the value of α to search the best results. Thus, we set $\alpha = 5$ in all the experiments.

Influence of ID-OOD boundary refinement. Also, we conduct ablation study on the ID-OOD Boundary Refinement module. Table 5 illustrates the ablation results on the Charades-STA dataset. Obviously, when $\Delta = 0.04$, we can obtain the best performance.

Analysis on cross-modal interaction. As shown in Table 6, we further evaluate the importance of three components in the cross-modal interaction module: video-query matching, frame-query matching and positive-unlabeled learning. We find that the video-query matching component achieves the largest improvement, which is because wrong video-query matching will directly lead to retrieval failure. Moreover, positive-unlabeled learning brings significant improvement since it can recognize the proper moment proposals by the binary cross-entropy loss. In addition, frame-query matching provides fine-grained vision-language alignment for more precise retrieval. Thus, all three components in our cross-modal interaction module are significant.

Parameter analysis. As shown in Table 7, we conduct experiments on the ActivityNet Captions dataset under the open-set setting, and present the ablation study on the hyper-parameters ($\lambda_1, \lambda_2, \lambda_3, \eta$). We can find that, their performance only varies in a small range, indicating that our model is insensitive to these parameters. Finally, we choose $\lambda_1 = 0.6, \lambda_2 = 0.3, \lambda_3 = 0.7, \eta = 0.2$.

5 Conclusion

In this paper, we pose a brand-new and challenging task: open-set video moment retrieval (OS-VMR). Given a video and a query, the OS-VMR task aims to conduct retrieval if the query is video-relevant, otherwise reject the query. To address it, we propose a novel method for this special task. Experiments on three challenging benchmarks demonstrate the effectiveness of our method.

References

- [1] Jessa Bekker and Jesse Davis. 2020. Learning from positive and unlabeled data: A survey. *Machine Learning* 109, 4 (2020), 719–760.
- [2] Fuyao Cai, Daizong Liu, Xiang Fang, Jixiang Yu, Keke Tang, and Pan Zhou. 2025. Imperceptible Beam-Sensitive Adversarial Attacks for LiDAR-based Object Detection in Autonomous Driving. In *2025 IEEE International Conference on Multimedia and Expo (ICME)*. IEEE, 1–6.
- [3] Xiaowen Cai, Daizong Liu, Xiaoye Qu, Xiang Fang, Jianfeng Dong, Keke Tang, Pan Zhou, Lichao Sun, and Wei Hu. 2026. Towards building model/prompt-transferable attackers against large vision-language models. *Advances in Neural Information Processing Systems* 38 (2026), 174022–174058.
- [4] Joao Carreira and Andrew Zisserman. 2017. Quo vadis, action recognition? a new model and the kinetics dataset. In *CVPR*.
- [5] Jingyuan Chen, Xinpeng Chen, Lin Ma, Zequn Jie, and Tat-Seng Chua. 2018. Temporally grounding natural sentence in video. In *EMNLP*.
- [6] Jiaming Chen, Weixin Luo, Wei Zhang, and Lin Ma. 2022. Explore Inter-contrast between Videos via Composition for Weakly Supervised Temporal Sentence Grounding. In *AAAI*.
- [7] Long Chen, Chujie Lu, Siliang Tang, Jun Xiao, Dong Zhang, Chilee Tan, and Xiaolin Li. 2020. Rethinking the Bottom-Up Framework for Query-based Video Localization. In *AAAI*.
- [8] Zhenfang Chen, Lin Ma, Wenhan Luo, Peng Tang, and Kwan-Yee K Wong. 2020. Look closer to ground better: Weakly-supervised temporal grounding of sentence in video. *arXiv preprint arXiv:2001.09308* (2020).
- [9] Junyoung Chung, Caglar Gulcehre, KyungHyun Cho, and Yoshua Bengio. 2014. Empirical evaluation of gated recurrent neural networks on sequence modeling. In *NeurIPS*.
- [10] Ran Cui, Tianwen Qian, Pai Peng, Elena Daskalaki, Jingjing Chen, Xiaowei Guo, Huyang Sun, and Yu-Gang Jiang. 2022. Video Moment Retrieval from Text Queries via Single Frame Annotation. In *SIGIR*.
- [11] Laurent Dinh, David Krueger, and Yoshua Bengio. 2015. NICE: Non-linear independent components estimation. *ICLR* (2015).
- [12] Laurent Dinh, Jascha Sohl-Dickstein, and Samy Bengio. 2017. Density estimation using Real NVP. *International Conference on Learning Representations* (2017).
- [13] Wanlong Fang, Tianle Zhang, and Alvin Chan. 2026. To align or not to align: Strategic multimodal representation alignment for optimal performance. In *Proceedings of the AAAI Conference on Artificial Intelligence*, Vol. 40. 21056–21064.
- [14] Wanlong Fang, Tianle Zhang, Wen Tao, and Alvin Chan. 2026. Towards Understanding Modality Interaction in Multimodal Language Models via Partial Information Decomposition. In *International Conference on Machine Learning*.
- [15] Xiang Fang. 2026. Advancing Out-of-Distribution Detection Across Diverse Scenarios. In *Proceedings of the AAAI Conference on Artificial Intelligence*, Vol. 40. 41042–41043.
- [16] Xiang Fang, Arvind Easwaran, and Blaise Genest. 2025. Adaptive Multi-prompt Contrastive Network for Few-shot Out-of-distribution Detection. In *International Conference on Machine Learning*.
- [17] Xiang Fang, Arvind Easwaran, Blaise Genest, and Ponnuthurai Nagaratnam Suganthan. 2025. Adaptive Hierarchical Graph Cut for Multi-granularity Out-of-distribution Detection. *IEEE Transactions on Artificial Intelligence* (2025).
- [18] Xiang Fang, Arvind Easwaran, Blaise Genest, and Ponnuthurai Nagaratnam Suganthan. 2025. Your data is not perfect: Towards cross-domain out-of-distribution detection in class-imbalanced data. *Expert Systems with Applications* (2025).
- [19] Xiang Fang and Wanlong Fang. 2026. Disentangling Adversarial Prompts: A Semantic-Graph Defense for Robust LLM Security. In *Proceedings of the AAAI Conference on Artificial Intelligence*.
- [20] Xiang Fang and Wanlong Fang. 2026. SLAP: The Semantic Least Action Principle for Variational Video-Language Modeling. In *International Conference on Machine Learning*.
- [21] Xiang Fang, Wanlong Fang, and Wei Ji. 2026. Immuno-VLM: Immunizing Large Vision-Language Models via Generative Semantic Antibodies for Open-World Trustworthiness. In *International Conference on Machine Learning*.
- [22] Xiang Fang, Wanlong Fang, Wei Ji, and Tat-Seng Chua. 2025. Turing Patterns for Multimedia: Reaction-Diffusion Multi-Modal Fusion for Language-Guided Video Moment Retrieval. In *ACM International Conference on Multimedia*.
- [23] Xiang Fang, Wanlong Fang, and Changshuo Wang. 2025. Hierarchical Semantic-Augmented Navigation: Optimal Transport and Graph-Driven Reasoning for Vision-Language Navigation. In *Advances in Neural Information Processing Systems*.
- [24] Xiang Fang, Wanlong Fang, and Changshuo Wang. 2026. CogniVerse: Revolutionizing Multi-modal Retrieval-Augmented Generation with Cognitive Reflection and Geometric Reasoning. In *Proceedings of the IEEE/CVF Conference on Computer Vision and Pattern Recognition*.
- [25] Xiang Fang, Wanlong Fang, and Changshuo Wang. 2026. Unveiling the Fragility of Vision-Language Models: Multi-Modal Adversarial Synergy via Texture-Constrained Perturbations and Cross-Modal Optimization. In *Proceedings of the AAAI Conference on Artificial Intelligence*.
- [26] Xiang Fang, Wanlong Fang, Changshuo Wang, Daizong Liu, Keke Tang, Jianfeng Dong, Pan Zhou, and Beibei Li. 2025. Multi-pair temporal sentence grounding via multi-thread knowledge transfer network. In *Proceedings of the AAAI Conference on Artificial Intelligence*, Vol. 39. 2915–2923.
- [27] Xiang Fang, Wanlong Fang, Changshuo Wang, Daizong Liu, Keke Tang, Jianfeng Dong, Pan Zhou, and Beibei Li. 2025. Multi-Pair Temporal Sentence Grounding via Multi-Thread Knowledge Transfer Network. In *Proceedings of the AAAI Conference on Artificial Intelligence*.
- [28] Xiang Fang, Wanlong Fang, Changshuo Wang, Xiaoye Qu, and Daizong Liu. 2026. Rethinking Video-language Model From the Language Input Perspective. In *Proceedings of the AAAI Conference on Artificial Intelligence*.
- [29] Xiang Fang, Wanlong Fang, Changshuo Wang, Keke Tang, Daizong Liu, Siyi Wang, and Wei Ji. 2026. Towards Unified Vision-Language Models With Incomplete Multi-Modal Inputs. In *Proceedings of the AAAI Conference on Artificial Intelligence*.
- [30] Xiang Fang and Yuchong Hu. 2020. Double self-weighted multi-view clustering via adaptive view fusion. *arXiv preprint arXiv:2011.10396* (2020).
- [31] Xiang Fang, Yuchong Hu, Pan Zhou, and Dapeng Wu. 2021. Animc: A soft approach for autoweighted noisy and incomplete multiview clustering. *IEEE Transactions on Artificial Intelligence* 3, 2 (2021), 192–206.
- [32] Xiang Fang, Yuchong Hu, Pan Zhou, and Dapeng Oliver Wu. 2020. V3H: View variation and view heredity for incomplete multiview clustering. *IEEE Transactions on Artificial Intelligence* 1, 3 (2020), 233–247.
- [33] Xiang Fang, Yuchong Hu, Pan Zhou, and Dapeng Oliver Wu. 2021. Unbalanced incomplete multi-view clustering via the scheme of view evolution: Weak views are meat; strong views do eat. *IEEE Transactions on Emerging Topics in Computational Intelligence* 6, 4 (2021), 913–927.
- [34] Xiang Fang, Daizong Liu, Wanlong Fang, Pan Zhou, Yu Cheng, Keke Tang, and Kai Zou. 2023. Annotations Are Not All You Need: A Cross-modal Knowledge Transfer Network for Unsupervised Temporal Sentence Grounding. In *Findings of the Association for Computational Linguistics: EMNLP 2023*. 8721–8733.
- [35] Xiang Fang, Daizong Liu, Wanlong Fang, Pan Zhou, Zichuan Xu, Wenzheng Xu, Junyang Chen, and Renfu Li. 2024. Fewer Steps, Better Performance: Efficient Cross-Modal Clip Trimming for Video Moment Retrieval Using Language. In *Proceedings of the AAAI Conference on Artificial Intelligence*, Vol. 38. 1735–1743.
- [36] Xiang Fang, Daizong Liu, Pan Zhou, and Yuchong Hu. 2022. Multi-modal cross-domain alignment network for video moment retrieval. *IEEE Transactions on Multimedia* 25 (2022), 7517–7532.
- [37] Xiang Fang, Daizong Liu, Pan Zhou, and Guoshun Nan. 2023. You can ground earlier than see: An effective and efficient pipeline for temporal sentence grounding in compressed videos. In *Proceedings of the IEEE/CVF Conference on Computer Vision and Pattern Recognition*. 2448–2460.
- [38] Xiang Fang, Daizong Liu, Pan Zhou, Zichuan Xu, and Ruixuan Li. 2023. Hierarchical local-global transformer for temporal sentence grounding. *IEEE Transactions on Multimedia* (2023).
- [39] Xiang Fang, Zeyu Xiong, Wanlong Fang, Xiaoye Qu, Chen Chen, Jianfeng Dong, Keke Tang, Pan Zhou, Yu Cheng, and Daizong Liu. 2024. Rethinking Weakly-supervised Video Temporal Grounding From a Game Perspective. In *European Conference on Computer Vision*. Springer.
- [40] Jiyang Gao, Chen Sun, Zhenheng Yang, and Ram Nevatia. 2017. Tall: Temporal activity localization via language query. In *ICCV*.
- [41] Jialin Gao, Xin Sun, Mengmeng Xu, Xi Zhou, and Bernard Ghanem. 2021. Relation-aware Video Reading Comprehension for Temporal Language Grounding. In *EMNLP*. 3978–3988.
- [42] Junyu Gao and Changsheng Xu. 2021. Fast video moment retrieval. In *ICCV*.
- [43] Runzhou Ge, Jiyang Gao, Kan Chen, and Ram Nevatia. 2019. Mac: Mining activity concepts for language-based temporal localization. In *WACV*.
- [44] Denis Gudovskiy, Shun Ishizaka, and Kazuki Kozuka. 2022. Cflow-ad: Real-time unsupervised anomaly detection with localization via conditional normalizing flows. *IEEE Winter Conference on Application of Computer Vision* (2022).
- [45] Dan Guo, Kun Li, Bin Hu, Yan Zhang, and Meng Wang. 2024. Benchmarking Micro-action Recognition: Dataset, Method, and Application. *IEEE Transactions on Circuits and Systems for Video Technology* 34, 7 (2024), 6238–6252.
- [46] Dan Hendrycks and Kevin Gimpel. [n. d.]. A Baseline for Detecting Misclassified and Out-of-Distribution Examples in Neural Networks. In *ICLR*.

- [47] Yen-Chang Hsu, Yilin Shen, Hongxia Jin, and Zsolt Kira. 2020. Generalized odin: Detecting out-of-distribution image without learning from out-of-distribution data. In *CVPR*.
- [48] Jaedong Hwang, Seoung Wug Oh, Joon-Young Lee, and Bohyung Han. 2021. Exemplar-Based Open-Set Panoptic Segmentation Network. In *CVPR*.
- [49] Wei Ji, Renjie Liang, Lizi Liao, Hao Fei, and Fuli Feng. 2023. Partial annotation-based video moment retrieval via iterative learning. In *MM*.
- [50] Wei Ji, Renjie Liang, Zhedong Zheng, Wenqiao Zhang, Shengyu Zhang, Juncheng Li, Mengze Li, and Tat-seng Chua. 2023. Are binary annotations sufficient? video moment retrieval via hierarchical uncertainty-based active learning. In *CVPR*.
- [51] Wei Ji, You Qin, Long Chen, Yinwei Wei, Yiming Wu, and Roger Zimmermann. 2024. Mrtnet: Multi-resolution temporal network for video sentence grounding. In *ICASSP*.
- [52] KJ Joseph, Salman Khan, Fahad Shahbaz Khan, and Vineeth N Balasubramanian. 2021. Towards open world object detection. In *CVPR*.
- [53] Minjoon Jung, Youwon Jang, Seongho Choi, Joochan Kim, Jin-Hwa Kim, and Byoung-Tak Zhang. 2023. Overcoming Weak Visual-Textual Alignment for Video Moment Retrieval. *arXiv preprint arXiv:2306.02728* (2023).
- [54] Diederik P Kingma and Jimmy Ba. 2014. Adam: A method for stochastic optimization. *arXiv preprint arXiv:1412.6980* (2014).
- [55] Polina Kirichenko, Pavel Izmailov, and Andrew G Wilson. 2020. Why normalizing flows fail to detect out-of-distribution data. *NeurIPS* 33 (2020), 20578–20589.
- [56] Ryan Kiros, Yukun Zhu, Russ R Salakhutdinov, Richard Zemel, Raquel Urtasun, Antonio Torralba, and Sanja Fidler. 2015. Skip-thought vectors. *Advances in Neural Information Processing Systems (NIPS)* 28 (2015).
- [57] Ranjay Krishna, Kenji Hata, Frederic Ren, Li Fei-Fei, and Juan Carlos Niebles. 2017. Dense-captioning events in videos. In *ICCV*.
- [58] Mingjin Kuai, You Qin, Xiang Fang, Wei Ji, and Roger Zimmermann. 2026. Dynamic Graph-enhanced Event Refinement for Temporal Sentence Grounding of Micro-moments. *IEEE Transactions on Multimedia* (2026).
- [59] Nishant Kumar, Siniša Šegvić, Abouzar Eslami, and Stefan Gumhold. 2023. Normalizing Flow based Feature Synthesis for Outlier-Aware Object Detection. In *CVPR*.
- [60] Kimin Lee, Kibok Lee, Honglak Lee, and Jinwoo Shin. 2018. A simple unified framework for detecting out-of-distribution samples and adversarial attacks. *NeurIPS* 31 (2018).
- [61] Huashuo Lei, Xiaowen Cai, Daizong Liu, Xiang Fang, Xiaoye Qu, Jianfeng Dong, Jixiang Yu, and Keyan Jin. 2025. Exploring Disentangled Appearance-Motion Contexts for Temporal Activity Localization. In *2025 International Joint Conference on Neural Networks (IJCNN)*. IEEE, 1–8.
- [62] Hongxiang Li, Meng Cao, Xuxin Cheng, Yaowei Li, Zhihong Zhu, and Yuexian Zou. 2023. G2l: Semantically aligned and uniform video grounding via geodesic and game theory. In *ICCV*.
- [63] Pandeng Li, Chen-Wei Xie, Hongtao Xie, Liming Zhao, Lei Zhang, Yun Zheng, Deli Zhao, and Yongdong Zhang. 2023. MomentDiff: Generative Video Moment Retrieval from Random to Real. In *NeurIPS*.
- [64] Ke Liang, Lingyuan Meng, Meng Liu, Yue Liu, Wenxuan Tu, Siwei Wang, Sihang Zhou, Xinwang Liu, Fuchun Sun, and Kunlun He. 2024. A survey of knowledge graph reasoning on graph types: Static, dynamic, and multi-modal. *TPAMI* (2024).
- [65] Ke Liang, Lingyuan Meng, Sihang Zhou, Wenxuan Tu, Siwei Wang, Yue Liu, Meng Liu, Long Zhao, Xiangjun Dong, and Xinwang Liu. 2024. MINES: Message Intercommunication for Inductive Relation Reasoning over Neighbor-Enhanced Subgraphs. In *AAAI*.
- [66] Ke Liang, Sihang Zhou, Meng Liu, Yue Liu, Wenxuan Tu, Yi Zhang, Liming Fang, Zhe Liu, and Xinwang Liu. 2024. Hawkes-enhanced spatial-temporal hypergraph contrastive learning based on criminal correlations. In *AAAI*.
- [67] Ke Liang, Sihang Zhou, Yue Liu, Lingyuan Meng, Meng Liu, and Xinwang Liu. 2023. Structure guided multi-modal pre-trained transformer for knowledge graph reasoning. *arXiv* (2023).
- [68] Shiyu Liang, Yixuan Li, and R Srikant. 2018. Enhancing the reliability of out-of-distribution image detection in neural networks. In *ICLR*.
- [69] Zhijie Lin, Zhou Zhao, Zhu Zhang, Qi Wang, and Huasheng Liu. 2020. Weakly-supervised video moment retrieval via semantic completion network. In *AAAI*.
- [70] Chengliang Liu, Jie Wen, Xiaoling Luo, Chao Huang, Zhihao Wu, and Yong Xu. 2023. DICNet: Deep Instance-Level Contrastive Network for Double Incomplete Multi-View Multi-Label Classification. In *AAAI*.
- [71] Chengliang Liu, Jie Wen, Xiaoling Luo, and Yong Xu. 2023. Incomplete Multi-View Multi-Label Learning via Label-Guided Masked View- and Category-Aware Transformers. In *AAAI*.
- [72] Chengliang Liu, Jie Wen, Zhihao Wu, Xiaoling Luo, Chao Huang, and Yong Xu. 2023. Information Recovery-Driven Deep Incomplete Multiview Clustering Network. *IEEE TNNLS* (2023).
- [73] Daizong Liu, Xiaowen Cai, Junhao Dong, Zhongliang Guo, Xiaoye Qu, Runwei Guan, Xiang Fang, and Dengpan Ye. 2026. Attacking Gray-Box Large Vision-Language Models with Adaptive SVD-Structured Adversarial Alignment. In *International Conference on Machine Learning*.
- [74] Daizong Liu, Xiang Fang, Wei Hu, and Pan Zhou. 2023. Exploring optical-flow-guided motion and detection-based appearance for temporal sentence grounding. *IEEE Transactions on Multimedia* 25 (2023), 8539–8553.
- [75] Daizong Liu, Xiang Fang, Xiaoye Qu, Jianfeng Dong, He Yan, Yang Yang, Pan Zhou, and Yu Cheng. 2024. Unsupervised domain adaptive temporal sentence localization with mutual information maximization. In *Proceedings of the AAAI Conference on Artificial Intelligence*, Vol. 38. 3567–3575.
- [76] Daizong Liu, Xiang Fang, Pan Zhou, Xing Di, Weining Lu, and Yu Cheng. 2023. Hypotheses tree building for one-shot temporal sentence localization. In *Proceedings of the AAAI Conference on Artificial Intelligence*, Vol. 37. 1640–1648.
- [77] Daizong Liu and Wei Hu. 2022. Skimming, Locating, then Perusing: A Human-Like Framework for Natural Language Video Localization. In *ACM MM*.
- [78] Daizong Liu, Xiaoye Qu, Xing Di, Yu Cheng, Zichuan Xu Xu, and Pan Zhou. 2022. Memory-Guided Semantic Learning Network for Temporal Sentence Grounding. In *AAAI*.
- [79] Daizong Liu, Xiaoye Qu, Jianfeng Dong, Guoshun Nan, Pan Zhou, Zichuan Xu, Lixing Chen, He Yan, and Yu Cheng. 2024. Filling the Information Gap between Video and Query for Language-Driven Moment Retrieval. In *ACM MM*.
- [80] Daizong Liu, Xiaoye Qu, Jianfeng Dong, Pan Zhou, Yu Cheng, Wei Wei, Zichuan Xu, and Yulai Xie. 2021. Context-aware Biaffine Localizing Network for Temporal Sentence Grounding. In *CVPR*.
- [81] Daizong Liu, Xiaoye Qu, Xiang Fang, Jianfeng Dong, Pan Zhou, Guoshun Nan, Keke Tang, Wanlong Fang, and Yu Cheng. 2024. Towards robust temporal activity localization learning with noisy labels. In *Proceedings of the 2024 Joint International Conference on Computational Linguistics, Language Resources and Evaluation (LREC-COLING 2024)*. 16630–16642.
- [82] Daizong Liu, Xiaoye Qu, and Wei Hu. 2022. Reducing the Vision and Language Bias for Temporal Sentence Grounding. In *ACM MM*.
- [83] Daizong Liu, Xiaoye Qu, Xiao-Yang Liu, Jianfeng Dong, Pan Zhou, and Zichuan Xu. 2020. Jointly Cross-and Self-Modal Graph Attention Network for Query-Based Moment Localization. In *ACM MM*.
- [84] Daizong Liu, Xiaoye Qu, Yinzhen Wang, Xing Di, Kai Zou, Yu Cheng, Zichuan Xu, and Pan Zhou. 2022. Unsupervised Temporal Video Grounding with Deep Semantic Clustering. In *AAAI*.
- [85] Daizong Liu, Mingyu Yang, Xiaoye Qu, Pan Zhou, Xiang Fang, Keke Tang, Yao Wan, and Lichao Sun. 2024. Pandora's box: Towards building universal attackers against real-world large vision-language models. *Advances in Neural Information Processing Systems* 37 (2024), 52127–52158.
- [86] Daizong Liu, Pan Zhou, Zichuan Xu, Haozhao Wang, and Ruixuan Li. 2022. Few-Shot Temporal Sentence Grounding via Memory-Guided Semantic Learning. *TCSVT* (2022).
- [87] Daizong Liu, Jiahao Zhu, Xiang Fang, Zeyu Xiong, Huan Wang, Renfu Li, and Pan Zhou. 2023. Conditional video diffusion network for fine-grained temporal sentence grounding. *IEEE Transactions on Multimedia* 26 (2023), 5461–5476.
- [88] Meng Liu, Xiang Wang, Liqiang Nie, Xiangnan He, Baoquan Chen, and Tat-Seng Chua. 2018. Attentive moment retrieval in videos. In *SIGIR*.
- [89] Meng Liu, Xiang Wang, Liqiang Nie, Qi Tian, Baoquan Chen, and Tat-Seng Chua. 2018. Cross-modal moment localization in videos. In *ACM MM*.
- [90] Matthew McDermott, Lasse Hyldig Hansen, Haoran Zhang, Giovanni Angelotti, and Jack Gallfiant. 2024. A Closer Look at AUROC and AUPRC under Class Imbalance. *arXiv preprint arXiv:2401.06091* (2024).
- [91] Yifei Ming, Yiyou Sun, Ousmane Dia, and Yixuan Li. 2023. How to Exploit Hyperspherical Embeddings for Out-of-Distribution Detection?. In *ICLR*.
- [92] Niluthpol Chowdhury Mithun, Sujoy Paul, and Amit K Roy-Chowdhury. 2019. Weakly supervised video moment retrieval from text queries. In *CVPR*.
- [93] Jonathan Munro and Dima Damen. 2020. Multi-modal domain adaptation for fine-grained action recognition. In *CVPR*.
- [94] Guoshun Nan, Rui Qiao, Yao Xiao, Jun Liu, Sicong Leng, Hao Zhang, and Wei Lu. 2021. Interventional Video Grounding with Dual Contrastive Learning. In *CVPR*.
- [95] Alexander Neubeck and Luc Van Gool. 2006. Efficient non-maximum suppression. In *ICPR*.
- [96] Hugo Oliveira, Caio Silva, Gabriel LS Machado, Keiller Nogueira, and Jefersson A dos Santos. 2021. Fully convolutional open set segmentation. *Machine Learning* (2021), 1–52.
- [97] David Osowiecki, Gustavo A Vargas Hakim, Mehrdad Noori, Milad Cheraghlikhani, Ismail Ben Ayed, and Christian Desrosiers. 2023. TTTFlow: Unsupervised Test-Time Training with Normalizing Flow. In *WACV*.
- [98] Jeffrey Pennington, Richard Socher, and Christopher D Manning. 2014. Glove: Global vectors for word representation. In *EMNLP*.
- [99] Michaela Regneri, Marcus Rohrbach, Dominikus Wetzel, Stefan Thater, Bernt Schiele, and Manfred Pinkal. 2013. Grounding action descriptions in videos. *TACL* (2013).
- [100] Marcus Rohrbach, Michaela Regneri, Mykhaylo Andriuk, Sikandar Amin, Manfred Pinkal, and Bernt Schiele. 2012. Script data for attribute-based recognition of composite activities. In *ECCV*.

- [101] Joan Serrà, David Álvarez, Vicenç Gómez, Olga Slizovskaia, José F Núñez, and Jordi Luque. [n. d.]. Input Complexity and Out-of-distribution Detection with Likelihood-based Generative Models. In *ICLR*.
- [102] Gunnar A Sigurdsson, Gül Varol, Xiaolong Wang, Ali Farhadi, Ivan Laptev, and Abhinav Gupta. 2016. Hollywood in homes: Crowdsourcing data collection for activity understanding. In *ECCV*.
- [103] Joyeeta Singha, Amarjit Roy, and Rabul Hussain Laskar. 2018. Dynamic hand gesture recognition using vision-based approach for human-computer interaction. *NCA* (2018).
- [104] Yijun Song, Jingwen Wang, Lin Ma, Zhou Yu, and Jun Yu. 2020. Weakly-supervised multi-level attentional reconstruction network for grounding textual queries in videos. *arXiv preprint arXiv:2003.07048* (2020).
- [105] Keke Tang, Chao Hou, Weilong Peng, Xiang Fang, Zhize Wu, Yongwei Nie, Wenping Wang, and Zhihong Tian. 2025. Simplification is all you need against out-of-distribution overconfidence. In *Proceedings of the Computer Vision and Pattern Recognition Conference*. 5030–5040.
- [106] Keke Tang, Wenyu Zhao, Weilong Peng, Xiang Fang, Xiaodong Cui, Peican Zhu, and Zhihong Tian. 2024. Reparameterization head for efficient multi-input networks. In *ICASSP 2024–2024 IEEE International Conference on Acoustics, Speech and Signal Processing (ICASSP)*. IEEE, 6190–6194.
- [107] Engkarat Techapanurak, Masanori Suganuma, and Takayuki Okatani. 2020. Hyperparameter-free out-of-distribution detection using cosine similarity. In *ACCV*.
- [108] Du Tran, Lubomir Bourdev, Rob Fergus, Lorenzo Torresani, and Manohar Paluri. 2015. Learning spatiotemporal features with 3d convolutional networks. In *ICCV*.
- [109] Ashish Vaswani, Noam Shazeer, Niki Parmar, Jakob Uszkoreit, Llion Jones, Aidan N Gomez, Lukasz Kaiser, and Illia Polosukhin. 2017. Attention is all you need. In *NeurIPS*.
- [110] Changshuo Wang, Xiang Fang, and Prayag Tiwari. 2025. DyPolySeg: Taylor Series-Inspired Dynamic Polynomial Fitting Network for Few-shot Point Cloud Semantic Segmentation. In *Forty-second International Conference on Machine Learning*.
- [111] Changshuo Wang, Shuting He, Xiang Fang, Jiawei Han, Zhonghang Liu, Xin Ning, Weijun Li, and Prayag Tiwari. 2025. Point clouds meets physics: Dynamic acoustic field fitting network for point cloud understanding. In *Proceedings of the Computer Vision and Pattern Recognition Conference*. 22182–22192.
- [112] Changshuo Wang, Shuting He, Xiang Fang, Zhijian Hu, Jia-Hong Huang, Yixian Shen, and Prayag Tiwari. 2026. Reasoning beyond points: A visual introspective approach for few-shot 3d segmentation. *Advances in Neural Information Processing Systems* 38 (2026), 117394–117414.
- [113] Changshuo Wang, Shuting He, Xiang Fang, Weijun Li, Xingyu Gao, Zhonghang Liu, Prayag Tiwari, and Dimitrios Kanoulas. 2026. From Coarse to Fine: Deep Prototype Refinement Network for Few-Shot Point Cloud Semantic Segmentation. *International Conference on Machine Learning* (2026).
- [114] Changshuo Wang, Shuting He, Xiang Fang, Weijun Li, Yixian Shen, Mingkun Xu, Zhongtian Sun, and Prayag Tiwari. 2026. TopAdapter: Topology-Aware Prompt Tuning for Efficient Point Cloud Understanding. *International Conference on Machine Learning* (2026).
- [115] Changshuo Wang, Shuting He, Xiang Fang, Fangzhe Nan, and Prayag Tiwari. 2025. Seeing the Overlooked: Bio-Visual Inspired Weak Saliency Feedback Transformer for Person Re-identification. In *Proceedings of the 33rd ACM International Conference on Multimedia*. 3192–3201.
- [116] Changshuo Wang, Shuting He, Xiang Fang, Meiqing Wu, Siew-Kei Lam, and Prayag Tiwari. 2025. Taylor series-inspired local structure fitting network for few-shot point cloud semantic segmentation. In *Proceedings of the AAAI Conference on Artificial Intelligence*, Vol. 39. 7527–7535.
- [117] Changshuo Wang, Zhijian Hu, Xiang Fang, Zai Yang Yu, Yibin Wu, Mingkun Xu, Yusong Wang, Xingyu Gao, and Prayag Tiwari. 2026. Biologically-Inspired Evolutionary Domain Symbiosis for Few-shot and Zero-shot Point Cloud Semantic Segmentation. In *Proceedings of the AAAI Conference on Artificial Intelligence*, Vol. 40. 9666–9674.
- [118] Junyi Wang, Jinjiang Li, Guodong Fan, Yakun Ju, Xiang Fang, and Alex C Kot. 2025. Prototype-driven structure synergy network for remote sensing images segmentation. *IEEE Transactions on Geoscience and Remote Sensing* (2025).
- [119] Siyi Wang, Suman Dutta, Wei Jie Bryan Lee, Jerrie Feng, Xiang Fang, and Anupam Chattopadhyay. 2025. Reducing T-Depth and T-Count in Quantum Multiplication Using Compressor Primitives. In *Proceedings of the Great Lakes Symposium on VLSI 2025*. 35–40.
- [120] Weiyao Wang, Matt Feiszli, Heng Wang, and Du Tran. 2021. Unidentified Video Objects: A Benchmark for Dense, Open-World Segmentation. In *ICCV*.
- [121] Yuechen Wang, Jiajun Deng, Wengang Zhou, and Houqiang Li. 2021. Weakly supervised temporal adjacent network for language grounding. *TMM* (2021).
- [122] Zheng Wang, Jingjing Chen, and Yu-Gang Jiang. 2021. Visual co-occurrence alignment learning for weakly-supervised video moment retrieval. In *ACM MM*.
- [123] Zhenzhi Wang, Limin Wang, Tao Wu, Tianhao Li, and Gangshan Wu. 2022. Negative Sample Matters: A Renaissance of Metric Learning for Temporal Grounding. In *AAAI*.
- [124] Shaoning Xiao, Long Chen, Songyang Zhang, Wei Ji, Jian Shao, Lu Ye, and Jun Xiao. 2021. Boundary proposal network for two-stage natural language video localization. In *AAAI*.
- [125] Zeyu Xiong, Daizong Liu, Xiang Fang, Xiaoye Qu, Jianfeng Dong, Jiahao Zhu, Keke Tang, and Pan Zhou. 2024. Rethinking video sentence grounding from a tracking perspective with memory network and masked attention. *IEEE Transactions on Multimedia* 26 (2024), 11204–11218.
- [126] Hai Yan, Haijian Ma, Xiaowen Cai, Daizong Liu, Zenghui Yuan, Xiaoye Qu, Jianfeng Dong, Runwei Guan, Xiang Fang, Hongyang He, et al. 2026. Fit the distribution: Cross-image/prompt adversarial attacks on multimodal large language models. *Advances in Neural Information Processing Systems* 38 (2026), 75204–75247.
- [127] Guide Yang, Chao Hou, Weilong Peng, Xiang Fang, Yongwei Nie, Peican Zhu, and Keke Tang. 2025. EOOD: Entropy-based Out-of-distribution Detection. In *2025 International Joint Conference on Neural Networks (IJCNN)*. IEEE, 1–8.
- [128] Wenfei Yang, Tianzhu Zhang, Yongdong Zhang, and Feng Wu. 2021. Local correspondence network for weakly supervised temporal sentence grounding. *TIP* (2021).
- [129] Xun Yang, Fuli Feng, Wei Ji, Meng Wang, and Tat-Seng Chua. 2021. Deconstructed video moment retrieval with causal intervention. In *SIGIR*.
- [130] Yijun Yang, Ruiyuan Gao, and Qiang Xu. 2022. Out-of-distribution detection with semantic mismatch under masking. In *ECCV*. Springer, 373–390.
- [131] Jie-En Yao, Li-Yuan Tsao, Yi-Chen Lo, Roy Tseng, Chia-Che Chang, and Chun-Yi Lee. 2023. Local Implicit Normalizing Flow for Arbitrary-Scale Image Super-Resolution. In *CVPR*.
- [132] Xincheng Yao, Ruoqi Li, Jing Zhang, Jun Sun, and Chongyang Zhang. 2023. Explicit Boundary Guided Semi-Push-Pull Contrastive Learning for Supervised Anomaly Detection. In *CVPR*.
- [133] Xinli Yu, Mohsen Malmir, Xin He, Jiangning Chen, Tong Wang, Yue Wu, Yue Liu, and Yang Liu. 2021. Cross interaction network for natural language guided video moment retrieval. In *SIGIR*.
- [134] Yitian Yuan, Lin Ma, Jingwen Wang, Wei Liu, and Wenwu Zhu. 2019. Semantic Conditioned Dynamic Modulation for Temporal Sentence Grounding in Videos. In *NeurIPS*.
- [135] Yitian Yuan, Tao Mei, and Wenwu Zhu. 2019. To find where you talk: Temporal sentence localization in video with attention based location regression. In *AAAI*.
- [136] Alireza Zaeemzadeh, Niccolo Bisagno, Zeno Sambugaro, Nicola Conci, Nazanin Rahnavard, and Mubarak Shah. 2021. Out-of-distribution detection using union of 1-dimensional subspaces. In *CVPR*. 9452–9461.
- [137] Runhao Zeng, Haoming Xu, Wenbing Huang, Peihao Chen, Mingkui Tan, and Chuang Gan. 2020. Dense regression network for video grounding. In *CVPR*.
- [138] Da Zhang, Xiyang Dai, Xin Wang, Yuan-Fang Wang, and Larry S Davis. 2019. Man: Moment alignment network for natural language moment retrieval via iterative graph adjustment. In *CVPR*.
- [139] Hao Zhang, Aixin Sun, Wei Jing, Liangli Zhen, Joey Tianyi Zhou, and Rick Siow Mong Goh. 2021. Natural language video localization: A revisit in span-based question answering framework. *IEEE TPAMI* (2021).
- [140] Hao Zhang, Aixin Sun, Wei Jing, and Joey Tianyi Zhou. 2020. Span-based Localizing Network for Natural Language Video Localization. In *ACL*.
- [141] Mingxing Zhang, Yang Yang, Xinghan Chen, Yanli Ji, Xing Xu, Jingjing Li, and Heng Tao Shen. 2021. Multi-stage aggregated transformer network for temporal language localization in videos. In *CVPR*. 12669–12678.
- [142] Songyang Zhang, Houwen Peng, Jianlong Fu, and Jiebo Luo. 2020. Learning 2D Temporal Adjacent Networks for Moment Localization with Natural Language. In *AAAI*.
- [143] Xiayue Zhang, Huashuo Lei, Daizong Liu, Xiaoye Qu, Xiang Fang, Runwei Guan, and Keyan Jin. 2025. Manipulating the Bounding Box: Multimodal Controlled Backdoor Attacks on 3D Visual Grounding Models. In *2025 International Joint Conference on Neural Networks (IJCNN)*. IEEE, 1–8.
- [144] Xiayue Zhang, Huashuo Lei, Daizong Liu, Xiaoye Qu, Xiang Fang, Runwei Guan, and Keyan Jin. 2025. MonoAttack: A Strong Attack Framework with Depth-Migration and Attribute-Tampering for Monocular 3D Object Detection. In *2025 International Joint Conference on Neural Networks (IJCNN)*. IEEE, 1–8.
- [145] Zhu Zhang, Zhijie Lin, Zhou Zhao, and Zhenxin Xiao. 2019. Cross-modal interaction networks for query-based moment retrieval in videos. In *SIGIR*.
- [146] Zhu Zhang, Zhou Zhao, Zhijie Lin, Xiuqiang He, et al. 2020. Counterfactual Contrastive Learning for Weakly-Supervised Vision-Language Grounding. *NeurIPS* (2020).
- [147] Yue Zhao, Yuanjun Xiong, Limin Wang, Zhirong Wu, Xiaoou Tang, and Dahua Lin. 2017. Temporal action detection with structured segment networks. In *ICCV*.
- [148] Minghang Zheng, Yanjie Huang, Qingchao Chen, Yuxin Peng, and Yang Liu. 2022. Weakly Supervised Temporal Sentence Grounding With Gaussian-Based Contrastive Proposal Learning. In *CVPR*. 15555–15564.
- [149] Yibo Zhou. 2022. Rethinking reconstruction autoencoder-based out-of-distribution detection. In *CVPR*. 7379–7387.